Traditional vs. sliding-joint masonry infilled frames: Seismic reliability and EAL

Available online at www.sciencedirect.com

ScienceDirect

Procedia Structural Integrity 26 (2020) 383–392

Structural Integrity Procedia

www.elsevier.com/locate/procedia

The 1st Mediterranean Conference on Fracture and Structural Integrity, MedFract1

Traditional vs. sliding-joint masonry infilled frames: Seismic reliability and EAL

F. Di Trapani[a]*, V. Bolis[b], F. Basone[c], L. Cavaleri[d] , M. Preti[b]

[a]*Politecnico di Torino. Dipartimento di Ingegneria Strutturale, Edile e Geotecnica*
[b]*Università degli Studi di Brescia. Department of Civil, Environmental, Architectural Engineering and Mathematics. Via Branze 43, 25123 Brescia, Italy*
[c]*Università degli Studi di Enna "Kore". Facoltà di Ingegneria e Architettura*
[d]*Università degli Studi di Palermo. Dipartimento di Ingegneria*

Abstract

In reinforced concrete (RC) multi-storey buildings, the important role of the seismic interaction of structural frames with masonry infills has been revealed by several earthquakes and investigated by many authors. Recently, several innovative infill solutions have been proposed to mitigate such interaction, which could result in widespread damage in both the masonry and the RC structure and sometimes jeopardize the building stability and the occupants' safety. One solution consists in the partitioning of the masonry infill into several sub-panels, relatively sliding along specific joints. This paper investigates the seismic assessment of this technological solution in the framework of performance based earthquake engineering. A two-dimensional five-storey RC seismic-resistant frame is selected as case study and the performance is assessed by comparing the responses of the same structure infilled with different solutions, made of sliding joints or traditional masonry, or in the bare configuration. Incremental Dynamic Analyses (IDA) is used for the probabilistic determination of fragility curves of the structures. Results show the seismic fragility and reliability of the different investigated structures, especially addressing the probabilities of occurrence of damage at different limit states and quantifying the associated expected annual loss.

Keywords: Seismic reliability; sliding-joints infills; expected annual loss; infilled frames; performance based earthquake engineering.

* Corresponding author. Tel.: +39-011-090-5323; fax: +39-011-090-5323.
E-mail address: fabio.ditrapani@polito.it

10.1016/j.prostr.2020.06.049

1. Introduction

Post-earthquake damage analyses have shown that a consistent part of the reparation costs of reinforced concrete (RC) buildings is related to reparation and/or strengthening of masonry infills and partition walls (Braga et al., 2011, De Martino et al., 2017, Del Vecchio et al., 2018), which generally suffer significant damage even in the case of moderate earthquakes. In fact, despite their effectiveness in terms of thermal, acoustic, fire and durability performance, traditional masonry infills are characterized by a large in-plane strength and stiffness, combined with a marked brittleness. As a consequence, they could reach their peak strength for low deformation levels, typically induced by moderate intensity earthquakes, thereafter, as the imposed drift increases, infills show in-plane and out-of-plane response degradation, with diffuse cracking and local crushing. In several cases this may evolve into infills out-of-plane collapse, which significantly increases risk for human life (Asteris et al., 2017, Di Trapani et al., 2018). Moreover, as shown in many studies (Preti et al., 2017, Cavaleri et al. 2017, and among others), traditional infills entail large interaction with the surrounding frame, inducing localized trusts on the frame columns, which could jeopardize their local performance.

Several studies have been carried out in the last decade in order to develop innovative infill solutions capable of undergoing limited damage when subjected to different levels of interstorey drifts demanded by earthquakes. They can be summarized into two main categories, one providing infill-frame system strengthening (e.g. Koutromanos et al., 2013), the other providing the reduction of infill-frame interaction (Preti et al., 2016, Preti et al., 2018). Among the latter, the partitioning of masonry infills with horizontal sliding joints has shown to be an effective solution for reducing infill-frame interaction and limiting the damage to infills even in the case of severe earthquakes. Such technique has been experimentally confirmed (Preti et al., 2016, Gao et al., 2018, Palios et al., 2017) and investigated in depth by parametric analyses (Bolis et al., 2017) that allowed providing a simplified equivalent strut modelling approach effectively describing the in-plane sliding-joints infilled frame response (Preti et al., 2017).

In order to assess the potential of the proposed innovative construction technique for the infills in RC framed structures, in the present paper, its seismic performance is compared with that of a traditional masonry infill, within a probabilistic assessment framework merging seismic fragility, reliability and loss assessment during the service life. The study adopts a performance based earthquake engineering (PBEE) approach, which can provide a quantification of the actual gain obtainable by adopting such kind of technological solution. The structural assessment is based on incremental dynamic analysis (IDA) (Vamvatsikos et al., 2002) for the determination of fragility curves, specifically defined in order to include limit states at structural and non-structural level. IDA are performed considering a selection of 30 ground motion records scaled, for the different systems, by assuming spectral acceleration at each specified vibration period, $S_a(T_1)$, as intensity measure (IM). Once obtained the fragility curves for the different structural systems, the assessment is moved to reliability by evaluating probabilities of exceeding each limit state. The analysis results are finally used to extend the investigation in terms of expected annual loss associated to each specified limit state, thus allowing the estimation of post-earthquake resto-ration costs within the service life.

2. Performance based earthquake engineering assessment framework

The PBEE framework is specifically designed to assess seismic performance of infilled frame systems, characterized by different infill configurations. As described by different authors (Cornell et al., 2000, Basone et al., 2019, Cavaleri et al., 2012), performance based earthquake engineering framework is generally made of four main steps: structural analysis, hazard analysis, damage analysis, and loss analysis.

The structural response is obtained by means of the IDA method, which has been recently widely employed by different authors (e.g. Basone et al., 2017, Di Trapani and Malavisi, 2019, and among others) to obtain a statistical distribution of the intensity measures inducing a limit state, taking into account the ground motions variability. For the IDAs, a set of 30 spectrum-compatible ground motions is selected and scaled in amplitude up to the achievement of the specified limit states defined as: (*i*) achievement of structural collapses during the analyses or (*ii*) limit values of engineering demand parameters (EDPs) (e.g. maximum interstorey drifts). In the adopted framework, for each analyzed structure characterized by its own fundamental vibration period (T_1), the selected ground motions are scaled with respect to the spectral acceleration attained in correspondence of T_1, to obtain $S_a(T_1)$ as a common value for each spectrum. The obtained spectra, and the associated records, are then scaled to be adopted as input ground motion in time history analyses.

From IDA results fragility curves for each limit state (defined in the following) can be derived, which express the probability of exceeding a specified limit state as a function of a specified *IM*, quantified by the following expression:

$$P\left[C \le D \mid IM = x\right] = \Phi\left(\frac{\ln(x) - \mu_{\ln_x}}{\sigma_{\ln_x}}\right) \tag{1}$$

Where $P[C \le D|IM=x]$ is the probability that a ground motion with $IM=x$ will cause the achievement of a limit state, Φ is the standard cumulative distribution function, $ln(x)$ is the natural logarithm of the variable x representing the intensity measure ($S_a(T_1)$) and μ_{lnX} and σ_{lnX} are the mean and the standard deviation of the natural logarithms of the distribution of x, respectively.

Based on fragility curves, reliability analysis can be performed to evaluate the probability (P_f) of exceeding a given limit state in a reference time period (in years), as expressed in Eq. (2).

$$P_f = \int_0^{+\infty} P\left[C \le D \mid IM = x\right] P\left[x\right] dx \tag{2}$$

where $P[x]$ is the probability of exceeding an $IM=x=S_a(T_1)$ in a specific site in the reference period (50 years) described by a Poisson model.

Hazard curves are obtained from the hazard analysis of the site, in which spectral ordinates at different vibration periods ($S_a(T_{1,i})$) are calculated for different annual rates of exceedance (λ), defined as the inverse of the return periods ($\lambda = 1/T_R$). As shown in Fig.1a, since fragility curves are referred to structures with different fundamental periods, a higher fragility not necessarily means higher probability of failure. Under this observation, the evaluation of P_f allows making consistent comparison between structural systems characterized by different vibration periods.

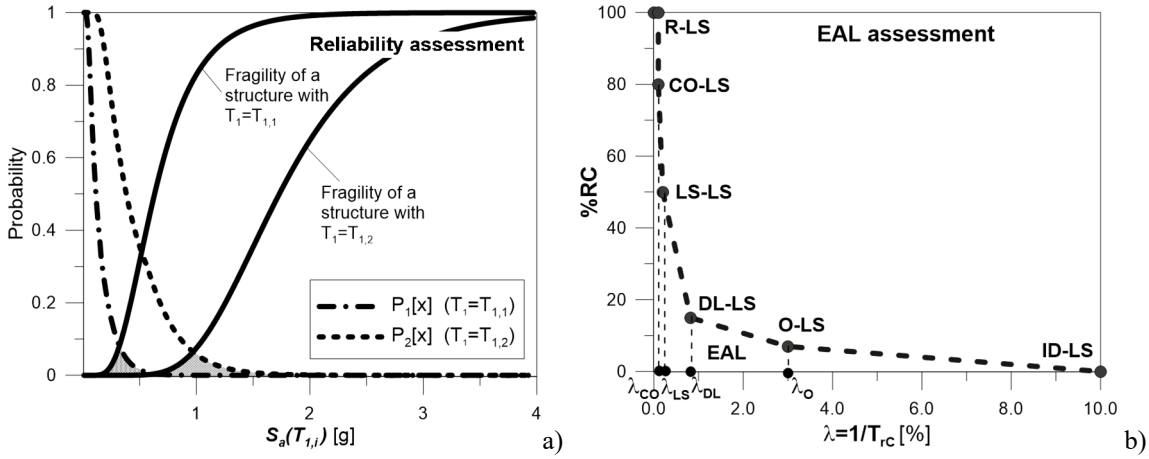

Fig. 1. Samples of reliability assessment of two structures having periods T_1 and T_2 (a) and typical EAL curve achievable from the reliability assessment (b).

The last stage of the PBEE framework consists in the evaluation of the expected annual loss (*EAL*) (Calvi 2013, Cosenza et al., 2018). EAL is determined starting from the performance of the structure for each limit state in terms of annual frequency of exceedance ($\lambda_{LS}=1/T_{rC\text{-}LS}$), being $T_{rC\text{-}LS}$ the capacity return period) and the associated repair costs, expressed as a fraction of reconstruction costs (*%RC*). In the proposed framework, the repair costs associated with each limit states have been assumed as those calibrated in Cosenza et al., 2018: the %RC associated with operational limit state (*O-LS*), damage limit state (*DL-LS*), life safety limit state (*LS-LS*) and collapse limit state (*CO-LS*) are 7%, 15%, 50% and 80%, respectively.

3. The reference case study structure

A 3-bays 5-stories RC frame extracted from a typical Italian residential building (plan view in Fig. 2a) is selected as reference structure for the present study. The frame (Fig. 2b) is designed according to the Italian building code meeting the design requirements for high ductility class. Concrete is supposed having nominal strength f_c=25 MPa, while steel rebars have nominal yielding strength f_y=560 MPa. The design of horizontal seismic forces is carried out using the design response spectrum obtained for the city of Cosenza (Italy) (soil type C) scaled by a 5.85 behavior factor.

Three different configurations for the frame are considered in the following analyses: bare frame (BF), fully infilled frame with traditional masonry infills (TI) and fully infilled frame with infills partitioned by horizontal sliding joints (SJ). For the sake of simplicity, no openings are assumed in the infills, whose effect would modify the response of both traditional (Asteris et al., 2016) and sliding joints (Bolis et al., 2019) solid infills. Both the typologies of masonry infills are made of clay hollow blocks with a thickness (t) of 200 mm and 15 mm. Sliding infills have horizontal sliding joints arranged as proposed by Preti et al., 2016 with the introduction of wooden boards able to activate the sliding between two adjacent masonry sub-portions.

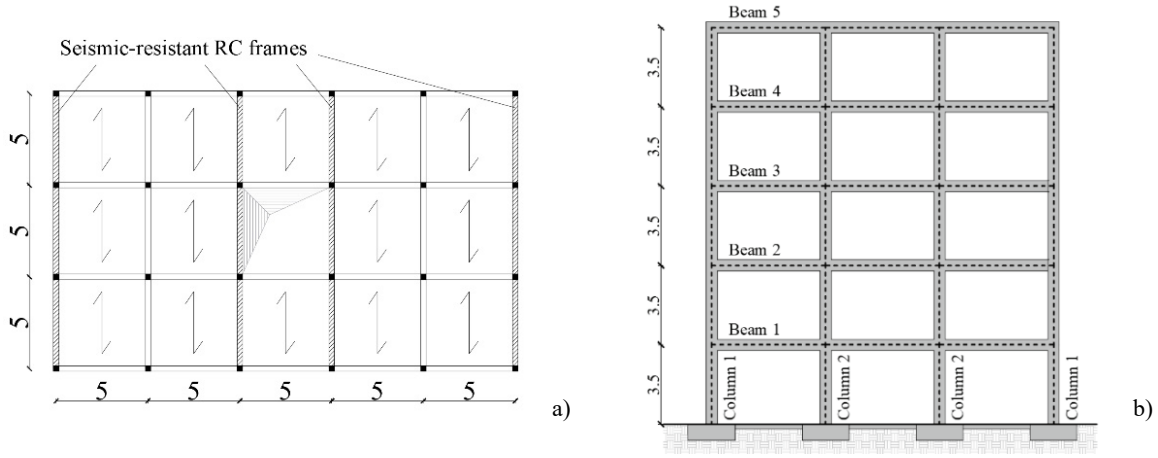

Fig. 2. Reference case study building: a) plan view; b) selected frame.

4. Modeling of the structure and limit states definition

4.1. Modeling of the infilled RC frame

IDAs on the reference structure have been performed with the *OpenSees* software platform (McKenna et al., 2000). A distributed plasticity approach is adopted to model the RC frame, using fiber-section beam-column elements characterized by the *Concrete04* material stress-strain model for the cross-section fibers. Confinement of concrete is accounted for by dividing cross-sections into effectively confined core fiber and unconfined cover fibers and elements into constant-confinement segments (Campione et al., 2016, Campione et al., 2017, Minafò et al., 2016) in such a way to account for the different transversal reinforcement, while steel rebars are included by means of the *Steel02* material model. The triggering of shear non-linear mechanism is not directly modeled, but possible shear damage or collapses in the frame elements are evaluated a-posteriori.

For the traditional infill, a double strut configuration is adopted. It provides two parallel struts per each infill diagonal, which are eccentric with respect to the beam-columns joints. The calibration of the struts inelastic response is based on the procedure proposed by Di Trapani et al., 2018.

As shown in Fig.3a, infill with sliding joints are modelled with two alternative compression-only struts hinged on the columns at a specified distance (z) from the frame joint, as proposed by Preti et al., 2017. The calibration of the strut is based on expressions, allowing, at each deformation level, the simultaneous prediction of the infill lateral strength (ΔF_s) and maximum shear in the columns ($V_{\max}^{col}$), which can be estimated by means of simple equilibrium

considerations based only on the geometric and material parameters of the infill. In detail, the axial stress-strain law of each strut is obtained by means of three axial springs in parallel, calibrated in order to reproduce the analytically obtained force-displacement response (Fig. 3b) and the typical cyclic response of the considered infill typology.

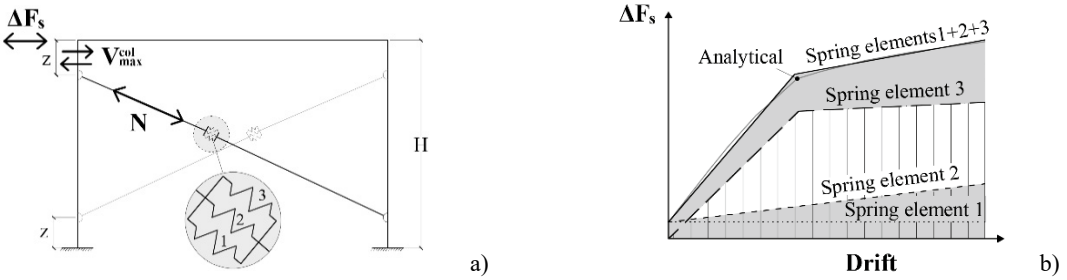

Fig. 3. Simplified equivalent strut model for the infills with horizontal sliding joints: a) equivalent strut model for the infill with horizontal sliding joints; b) force-drift relationships of springs.

4.2. Definition of structural and non-structural limit states

In the assessment framework the four standard PBEE limit states (namely operational limit state (O-LS), damage limitation limit state (DL-LS), life-safety limit state (LS-LS) and collapse limit state (CO-LS)) are considered. Two additional limit states are added to better characterize the different damage states. One concerns the frame initial damage (FID-LS) due to first yielding or first shear cracking, the other considers the attainment of infills severe damage (ISD-LS). Among the considered limit states, O-LS, DL-LS and ISD-LS are referred to damage of non-structural components (the infills), while FID-LS, LS-LS and CO-LS identify damage of structural elements.

The criteria adopted to define the different limit states are summarized in Table 1. As regards non-structural limit states, O-LS, DL-LS and ISD-LS are defined as function of the interstorey drift, based on the results previous experimental studies on traditional (Morandi et al., 2018) and sliding-joints infills (Preti et al., 2016, Preti et al., 2018, Gao et al., 2018). For what concerns structural limit states, collapse limit state (CO-LS) is achieved in correspondence of the first of the following conditions: i) achievement of ultimate chord-rotation (θ_u) of columns (evaluated according to Eurocode 8), ii) achievement of ultimate shear capacity ($V_{R,u}$) of columns, iii) achievement of 6.5% interstorey drift, when second order effects could jeopardize the stability of the structure. In the performed analyses, an axial force-chord rotation (N-θ) interaction domain is considered, in order to take into account the variation of chord rotation capacity as a function of the variation of axial load on columns, as proposed by Di Trapani and Malavisi, 2019. The ultimate shear capacity $V_{R,u}$ of column is evaluated according to the Model Code 2010 expression.

The LS-LS is simply defined by the 80% of the respective θ_u and $V_{R,u}$ capacities at CO-LS. Finally, the FID-LS is related to the first occurring condition between column rebars yielding and initial shear cracking. The former condition is associated with the achievement of the yielding rotation (θ_y) of frame column, according to Eurocode 8, while the first shear cracking is associated with the achievement of the resistance $V_{R,i}$, evaluated using the expression proposed by Collins (1998).

Table 1. Structural and non-structural limit state thresholds for traditional and sliding joint infills.

		Limit state thresholds			Considered for EAL
	Limit state	Traditional infilf	Sliding-joints infill	Bare Frame	
Non-Structural Limit states	O-LS	IDR=0.20%	IDR=2.00%	-	Yes
	DL-LS	IDR=0.50%	IDR=3.00%	-	Yes
	ISD-LS	IDR=1.50%	IDR=4.00%	-	No
Structural Limit states	FID-LS	θ_y or $V_{1st\ crack}$			No
	LS-LS	$0.8\theta_u$ or $0.8V_{Rd}$			Yes
	CO-LS	θ_u or V_{Rd} or IDR=6.5%			Yes

5. Incremental dynamic analysis

As shown in Fig. 4, a set of 30 natural ground motions is selected through the software REXEL (Iervolino et al., 2009) in order to get spectrum-compatibility with the design spectrum of the site of Cosenza (Italy) with soil type C and 457 years return period.

To perform IDAs, accelerograms are scaled in such a way that the respective spectra assume the same value of $S_a(T_1)$ in correspondence to the first vibration period for each considered structure.

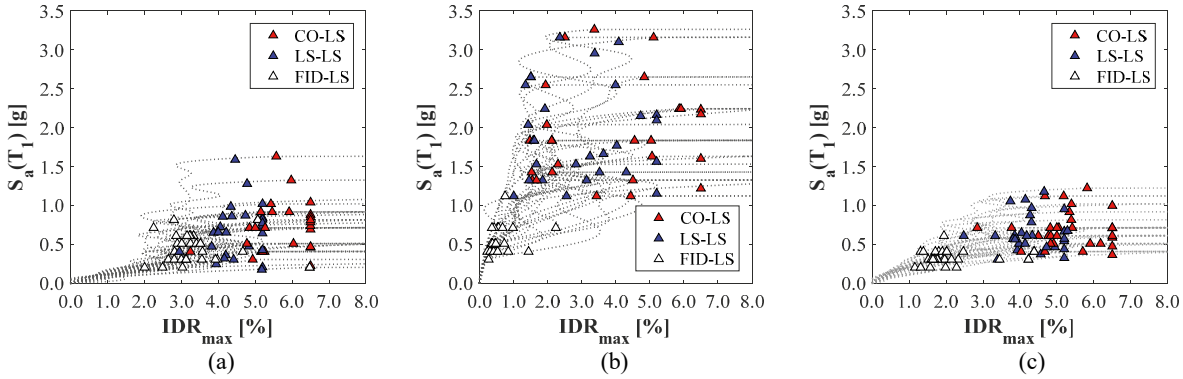

Fig. 4. IDA curves and structural limit state points for: a) bare frame, b) traditionally infilled frame; c) sliding-joint infilled frame.

IDA curves highlighting structural limit states are reported in Fig. 4. The overall trend shows that bare frame and sliding joint-infilled frame achieve collapse in correspondence of very similar spectral acceleration levels. Also maximum interstorey drifts recorded present similar magnitudes, ranging between 4.5% and 6.5%, which also demonstrate the trend of sliding-joint infilled frames to behave in a ductile manner with very few cases of shear collapse in the columns. A very different trend is observed for traditionally infilled frames, which present collapses at significantly higher spectral acceleration levels and noticeably reduced ultimate displacement values.

As regards frame initial damage limit state, the presence of the infill anticipates the damage activation in both the TI and the SJ case (occurred at about 0.5% and 1.5%, respectively), with respect to the BF one, for which the FID-LS is reached at about 3% drift. The difference between the performance of the two infilled configuration is related to the different stiffening effect acted by the two infill typologies.

6. Hazard, fragility and reliability assessment

For the site under investigation (Cosenza, Italy) and the specified soil stiffness (type C according to EC8 classification), hazard curves, representing the annual rates of exceeding the IM=$S_a(T_1)$, are obtained for each vibration period associated with the three structural typologies. The resulting hazard curves are superimposed with fragility curves of the three structural typologies (Figs. 5 and 6). The intersection areas between hazard and fragility curves are proportional to the probabilities of exceeding the different limit states, which are numerically determined by Eq. (2). Figs. 5 and 6 highlight the different amplitudes of the intersection areas between hazard and fragility curves, showing that, in the case of traditionally infilled frames, major intersection amplitudes can be recognized for both structural and non-structural limit states.

The obtained probabilities of occurrence (P_f) for both structural and non-structural limit states are reported in Table 2. From the structural point of view, noticeable differences can be observed for the FID-LS, where TI frames achieve a P_f of 15%, which results 5 times and 10 times the same probabilities evaluated for SJ infilled frame and bare frame respectively. As regards LS-LS and CO-LS, the obtained probabilities of occurrence are in the same order magnitude for the three cases, with the traditionally infilled frame presenting slightly larger values. However, the largest differences are highlighted from non-structural limit states, which show a significantly reduced probability of occurrence in the cases of SJ infills with respect to TI for all the considered LS. Probabilities of

occurrence of O-LS, DL-LS and ISD-LS for traditionally infilled frames are about 10 times, 13 times and 5 times the probabilities evaluated in the case sliding-joint infilled frames. This result can be justified by the reduced stiffness and shear interaction of SJ infills with the frame, which allows the attainment of non-structural LS at significantly larger drifts with respect to the case of TI frames. Moreover, the hazard for the SJ infilled frame is significantly lower than that of TI case, due to a longer vibration period, which is close to that of the bare frame.

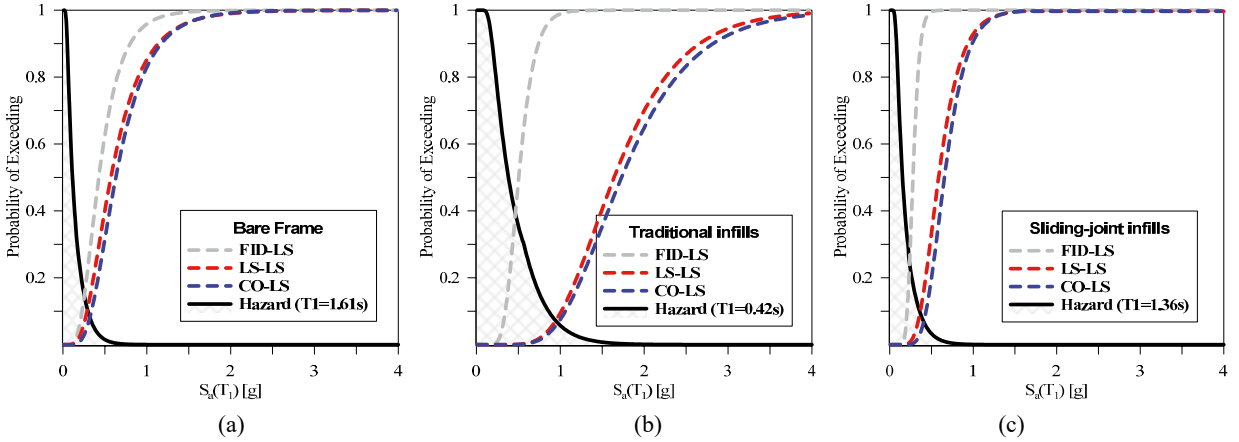

Fig. 5. Fragility curves of structural limit states and hazard curves (Cosenza, Soil Type C) for: a) bare frame; b) traditionally infilled frame; c) sliding-joint infilled frame.

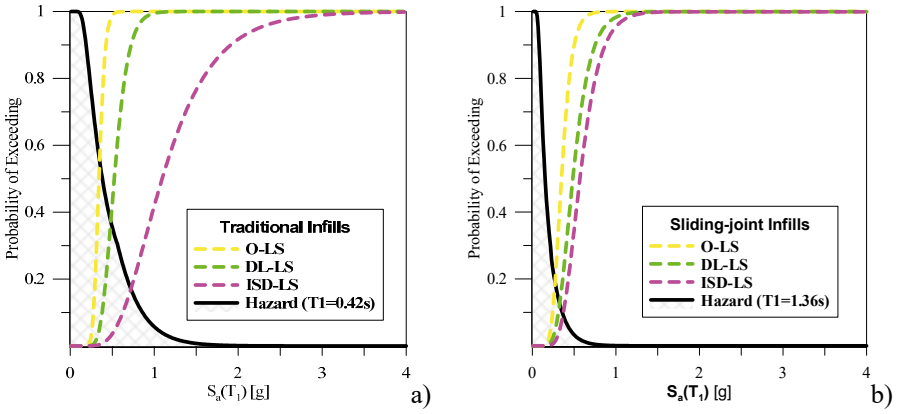

Fig. 6. Fragility curves of non-structural limit states and hazard curves (Cosenza, Soil Type C) for: a) traditionally infilled frame; b) sliding-joint infilled frame.

Table 2. Probabilities of occurrence of limit states for the different structures.

		Probabilities of failure P_f (-)		
		Bare Frame	Traditional Infills	Sliding-joint infills
Non-structural LS	O-LS	-	1.72×10^{-1}	1.60×10^{-2}
	DL-LS	-	9.53×10^{-2}	7.41×10^{-3}
	ISD-LS	-	2.23×10^{-2}	4.41×10^{-3}
Structural LS	FID-LS	1.48×10^{-2}	1.50×10^{-1}	2.50×10^{-2}
	LS-LS	3.92×10^{-3}	4.77×10^{-3}	4.45×10^{-3}
	CO-LS	2.49×10^{-3}	3.95×10^{-3}	2.61×10^{-3}

7. Loss assessment

Expected annual loss assessment is carried out using the procedure by Cosenza et al., 2018, updated as illustrated in section 2 and considering only the standard limit states for structural components (LS-LS and CO-LS) and non-structural components (O-LS and DL-LS). λ_{LS} and $\overline{S}_{a-LS}(T_1)$ values are reported in Table 3, while Fig. 7 illustrates the obtained λ-%RC relationships for TI and SJ cases. The obtained expected annual loss of the sliding-joint infilled frame (0.40%) is about half of the traditionally infilled frame (0.76%). This difference is entirely due to the gain in terms of reduced λ for non-structural limit states, which is one order of magnitude lower with respect to the case of traditional infills. Both TI and SJ structures have EAL lower than the reference value of 1.13%, which is associated to the ideally code conforming building. This highlights that, traditionally infilled frames design according to seismic codes have adequate performance in terms of EAL, which allow assigning an A seismic risk class according to the Italian guidelines for seismic risk classification (Cosenza et al., 2018). On the other hand, the adoption of sliding-joint infills allows the achievement of the most preforming risk class (A+).

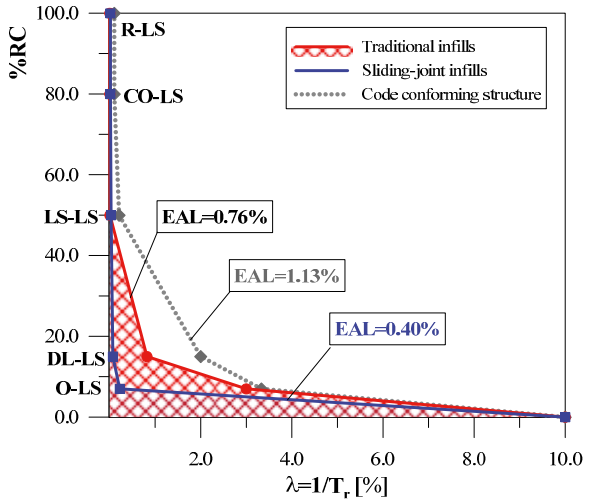

Fig. 7: λ-%RC relationships and EAL for TI frames, SJI frame and code compliant reference structure.

Table 3. $\overline{S}_{a-LS}(T_1)$ and λ_{LS} values at the different limit states and EAL values for TI frames and SJI frames.

	Traditional Infills			Sliding-joint infills		
	$\overline{S}_{a-LS}(T_1)$[g]	λ_{LS}	EAL [%]	$\overline{S}_{a-LS}(T_1)$[g]	λ_{LS}	EAL [%]
CO-LS	1.73	5.76×10^{-5}		0.66	1.84×10^{-4}	
LS-LS	1.64	8.36×10^{-5}	0.76	0.59	3.24×10^{-4}	0.40
DL-LS	0.52	8.21×10^{-3}		0.49	7.27×10^{-4}	
O-LS	0.34	1.69×10^{-2}		0.35	2.25×10^{-3}	

8. Conclusions

The paper presented a PBEE approach properly defined to assess and compare the performance of infilled frames with traditional infills and innovative infills with sliding-joint sub-panels. The adopted methodology is based on incremental dynamic analysis performed considering specific limit states defined to account for both structural and non-structural damage. The performances of the systems are compared through a reliability assessment carried out by accounting for both fragility and hazard to obtain probabilities of occurrence of each considered limit state.

The IDA curves show that the frame infilled with the innovative sliding joint technique tends to behave similarly to the bare frame in terms of strength, stiffness and failure modes. On the contrary, the response of traditionally

infilled frame is characterized by significantly increased overall resistance but, in many cases, brittle shear failures due to the large shear demand related to the stronger infill-frame interaction. As for the non-structural limit states, their attainment is significantly delayed in SJ frames (in terms of interstorey drift) because of the reduced tendency to undergo severe damage even in case of large interstorey drifts.

Although fragility curves of TI frames apparently show a significantly better performance, similar probabilities of occurrence (P_f) have been obtained for life safety and collapse limit-states for the three considered cases. On the contrary, large reliability differences are observed for non-structural limit states, where P_f of O-LS, DL-LS and ISD-LS for traditionally infilled frames was about 10 times, 13 times and 5 times the same probabilities evaluated in for SJI frames. Such reliability differences are due to the lower damage suffered by SJ infills with respect to TI frames, even for of large drifts, and also to the lower hazard associated with the longer vibration period of SJ infilled frames.

The performed expected annual loss assessment allows evaluating, for SJ infilled frames, an EAL equal to 0.40%, that is about a half of that of traditionally infilled frames (0.76%). This gain is entirely related to the reduced annual rates of exceeding evaluated for non-structural limit states in case of SJ infilled frames.

As a conclusion, the reported assessment highlights that frames infilled with the sliding joints technique results an effective design solution to improve reliability and reduce losses during the service life of masonry infilled RC structures.

Acknowledgements

This study was supported by ReLUIS, Rete di Laboratori Universitari di Ingegneria Sismica, WP 10, 2019-2021.

References

Braga, F., Manfredi, V., Masi, A., Salvatori, A., Vona, M. Performance of non-structural elements in RC buildings during the L'Aquila, 2009 earthquake, Bull Earth Eng, 9(1), 307–324, 2011.

De Martino G., Di Ludovico, M., Prota, A., Moroni, C., Manfredi, G., Dolce, M. Estimation of repair costs for RC and masonry residential buildings based on damage data collected by post-earthquake visual inspection, Bull Earth Eng, 15(4),1681–1706, 2017.

Del Vecchio, C., Di Ludovico, M., Pampanin, S., Prota, A. Repair costs of existing RC buildings damaged by the L'Aquila earthquake and comparison with FEMA P-58 pre-dictions, Earthq Spectra, 34(1), 237–263, 2018.

Asteris, P.G., Cavaleri, L., Di Trapani, F., Tsaris, A.K. Numerical modelling of out-of-plane response of infilled frames: state of the art and future challenges for the equivalent strut macromodels, Eng Struct, 132, 110–122, 2017.

Di Trapani, F., Shing, P.B., Cavaleri, L. Macroelement Model for In-Plane and Out-of-Plane Responses of Masonry Infills in Frame Structures, J of Struct Eng, 144(2), 04017198, 2018.

Preti, M., Bolis, V. Seismic analysis of a multi-story RC frame with infills partitioned by sliding joints, Ingengeria Sismica, 34(3-4), 175–187, 2017.

Cavaleri, L., Di Trapani, F., Asteris, P.G., Sarhosis, V. Influence of column shear failure on pushover based assessment of masonry infilled reinforced concrete framed structures: a case study, Soil Dynamics and Earthquake Engineering, 100, 98–112, 2017.

Fiore, A., Spagnoletti, G., Greco, R. On the prediction of shear brittle collapse mechanisms due to the infill-frame interaction in RC buildings under pushover analysis, En Struct, 121, 147-159, 2016.

Greco, R., Fiore, A., Marano, G.C. The role of modulation function in nonstationary stochastic earthquake model, Journal of Earthquake and Tsunami, 8(5), 1450015, 2014.

Koutromanos, I., Kyriakides, M., Stavridis, A., Billington, S., Shing, P.B. Shake-table tests of a three-story masonry-infilled RC frame retrofitted with composite materials, J Struct Eng, 139(8), 1340-1351, 2013

Preti, M., Bolis, V., Stavridis, A. Design of masonry infill walls with sliding joints for earthquake structural damage control, Proceedings of the 16th International Brick and Block Masonry Conference, IBMAC, Padua, Italy, 2016.

Preti, M., Neffati, M., Bolis, V. Earthen masonry infill walls: Use of wooden boards as sliding joints for seismic resistance, Construction and Building Materials, 184, 100–110, 2018.

Gao, X., Stavridis, A., Bolis, V., Preti, M. Experimental study on the seismic performance of non-ductile rc frames infilled with sliding subpanels, Proccedings of Eleventh U.S. National Conference on Earthquake Engineering Integrating Science, Engineering & Policy, Los Angeles, California, 2018.

Palios, X., Fardis, M.N., Strepelias, E., Bousias, S.N. Unbonded brickwork for the protection of infills from seismic damage, Eng Struct, 131, 614–624, 2017.

Bolis, V., Stavridis, A., Preti, M. Numerical Investigation of the In-Plane Performance of Masonry-Infilled RC Frames with Sliding Subpanels, J Struct Eng, 143(2), 04016168, 2017.

Preti, M., Bolis, V., Stavridis, A. Seismic infill–frame interaction of masonry walls partitioned with horizontal sliding joints: analysis and simplified modeling, Journal of Earthquake Engineering, 1–27, 2017.

Vamvatsikos, D., Cornell, A.C. Incremental dynamic analysis, Earthq Eng Struct Dyn 31(3),491–514, 2002.

Cornell, C.A., Krawinkler, H. Progress and challenges in seismic performance assessment. PEER Center News 3, University of California, Berkeley, 2000.

Basone, F., Castaldo, P., Cavaleri, L., Di Trapani, F. Response spectrum analysis of frame structures: reliability-based comparison between complete quadratic combination and damping-adjusted combination, Bulletin of Earthquake Engineering, 17(5), 2687-2713, 2019.

Cavaleri, L., Di Trapani, F., Macaluso, G., Papia, M. Reliability of code proposed models for assessment of masonry elastic moduli, Ingegneria Sismica, 29(1), 38–59, 2012.

Basone, F., Cavaleri, L., Di Trapani, F., Muscolino, G. Incremental dynamic based fragility assessment of reinforced concrete structures: Stationary vs. non-stationary artificial ground motions. Soil Dynamics and Earthquake Engineering, 103, 105–117, 2017.

Di Trapani, F., Malavisi, M. Seismic fragility assessment of infilled frames subject to mainshock/aftershock sequences using a double incremental dynamic analysis approach, Bulletin of Earthquake Engineering, 17(1), 211-235, 2019

Calvi G.M. Choices and criteria for seismic strengthening. J Earthq Eng, 17, 769–802, 2013.

Cosenza, E., Del Vecchio, C., Di Ludovico, M., Dolce, M., Moroni, C., Prota, A., Renzi, E. The Italian guidelines for seismic risk classification of constructions: technical principles and validation, Bulletin of Earthquake Engineering, 16(12), 5905-5935, 2018.

Ministry Decree, January 17th, 2018. Norme tecniche per le costruzioni (Technical codes for construction) [in Italian], 2018.

Asteris, P.G., Cavaleri, L., Di Trapani, F., Sarhosis, V. A macro-modelling approach for the analysis of infilled frame structures considering the effects of openings and vertical loads, Structure and Infrastructure Engineering, 12(5), 551–566, 2016.

Bolis, V., Preti, M. Openigns in infills with horizontal sliding joints: a parametric study to support the design, Bulletin of Earthquake Engineering, Submitted for publication., 2019.

McKenna, F., Fenves, G.L., Scott, M.H. Open system for earthquake engineering simulation," University of California, Berkeley, CA, 2000.

Campione, G., Cavaleri, L., Di Trapani, F., Macaluso, G., Scaduto, G. Biaxial deformation and ductility domains for engineered rectangular RC cross-sections: a parametric study highlighting the positive roles of axial load, geometry and materials, Eng Struct, 107(15), 116–134, 2016.

Campione, G., Cavaleri, L., Di Trapani, F., Ferrotto, M.F. Frictional effects in structural behavior of no end-connected steel-jacketed RC columns: experimental results and new approaches to model numerical and analytical response, J Struct Eng, 143(8), 04017070, 2017.

Minafò, G., Di Trapani, F., Amato, G. Strength and ductility of RC jacketed columns: A simplified analytical method, Engineering Structures, 122, 184-195, 2016.

Di Trapani, F., Bertagnoli, G., Ferrotto, M.F., Gino, D. Empirical Equations for the Direct Definition of Stress–Strain Laws for Fiber-Section-Based Macromodeling of Infilled Frames, Journal of Engineering Mechanics, 144(11), 04018101, 2018.

Morandi, P., Hak, S., Magenes, G. Performance-based interpretation of in-plane cyclic tests on RC frames with strong masonry infills, Engineering Structures, 156, 503–521, 2018.

Fédération internationale du béton (FIB). Model code 2010: final draft, International Federation for Structural Concrete, 2012.

Collins M.P. Procedures for Calculating the Shear Response of Reinforced Concrete Elements: A Discussion, Journal of Structural Engineering, 124(12), 1485–1488, 1998.

Iervolino, I., Galasso, C., Cosenza, E. REXEL: computer aided record selection for code-based seismic structural analysis, Bull of Earthquake Eng, 8, 339-362, 2009.

Di Trapani, F., Bolis, V., Basone, F., Preti, M., 2020. Seismic reliability and loss assessment of RC frame structures with traditional and innovative masonry infills. Eng. Struct 208, 110306.

Di Trapani, F., Giordano L., Mancini, G., 2020. Progressive Collapse Response of Reinforced Concrete Frame Structures with Masonry Infills. J. Eng. Mech. 146(3), 04020002.

Di Trapani, F., Ferro, G.A., Malavisi, M., 2020. Definition of inelastic displacement demand spectra for precast industrial facilities with friction and fixed beam-to-column joints. Soil Dynamics and Earthquake Engineering 128, 105871.

Cavaleri, L., Di Trapani, F., Ferrotto, M.F., Davì, L., 2017. Stress-strain models for normal and high strength confined concrete: Test and comparison of literature models reliability in reproducing experimental results. Ingegneria Sismica 34(3-4), 114-137.

Cavaleri, L., Di Trapani, F., Ferrotto, M.F., 2017. A new hybrid procedure for the definition of seismic vulnerability in Mediterranean cross-border urban areas. Natural HazardsVolume 86, 517-541.

Gino, D., Bertagnoli, G., Mazza, D.L., Mancini, G., 2017. A quantification of model uncertainties in NLFE of R.C. shear walls subjected to repeated loading. Ingegneria Sismica 34 (3-4), 79-91.

Bertagnoli, G., Mancini, G., Tondolo, F., (2009). Numerical modelling of early age concrete hardening. Magazine of Concrete Research 61 (4), 299-307.